JOURNAL OF CHEMICAL ENGINEERING AND INDUSTRIAL BIOTECHNOLOGY
E-ISSN: 0126-8139
VOLUME 11, ISSUE 1, JULY 2025, 41 - 58
DOI: https://doi.org/10.15282/jceib.v11i1.12401

RESEARCH ARTICLE

Mathematical Modelling of Rare Earth Elements Recovery by Ion Exchange Leaching from Ion Adsorption Clays

Nurul Aniyyah Mohamad Sobri[1,2], Noorlisa Harun[1]*

[1] Faculty of Chemical and Process Engineering Technology, Universiti Malaysia Pahang Al-Sultan Abdullah, 26600 Pahang, Malaysia

[2] Natural Resources and Environment Department (Chemical), Faculty of Engineering Technology, Universiti College TATI, 24000 Kemaman, Terengganu, Malaysia

ABSTRACT - The establishment of a mathematical model for the ion exchange leaching process is key to creating a theoretical basis for the recovery of rare earth elements (REEs) from ion adsorption clay. Given the complexity of the process and limitations of experimental methods, modelling and simulation provide a promising, cost-effective approach to understanding ion exchange leaching mechanisms for REE extraction. Therefore, this study aims to develop a such a model, employing the Shrinking Core Model and utilizing $MgSO_4$ as the leaching solution. A kinetic model was successfully developed based on the rate-determining step equation which belonged to the internal diffusion control. The calculated k value was 0.005, and the initial n value of 1.53 was later modified to 1.33 due to a deviation exceeding 10% in the Normalized Root Mean Square Error (NRMSE) value. The statistical model validation demonstrated a high level of agreement with the index values of d = 0.978, indicating an excellent agreement with experimental data, and a low value of NRMSE = 7.9 %, indicating an excellent performance model. The model consistently exhibits exponential growth in REE leaching efficiency, eventually reaching a maximum of 100% as leaching time progresses, demonstrating the leaching behaviour of REE extraction observed in this model follow the patterns observed in the leaching experiment. In conclusion, the developed kinetic model has the potential to provide reliable data on REE leaching efficiency at different leaching times across various concentrations of $MgSO_4$ solution.

ARTICLE HISTORY
Received : 7th May 2025
Revised : 10th June 2025
Accepted : 11th July 2025
Published : 14th July 2025

KEYWORDS
Rare earth elements (REE)
Ion adsorption clay
REE leaching efficiency
Mathematical model
Magnesium sulphate
Shrinking Core Model

1. INTRODUCTION

Rare earth elements (REEs) are now essential in modern technology, playing critical roles in the development of a wide range of high-tech applications [1]–[3]. REEs are generally used in minimal quantities across various high-tech applications because of their remarkable ability to improve product performance, durability, and efficiency. [4]. Due to rising demand driven by advancing technologies such as hybrid and electric vehicles, magnets, and optical instruments, the REE metals market, which was estimated at USD 13.2 billion in 2019, is projected to expand at a compound annual growth rate (CAGR) of about 10.7% from 2020 to 2026 [5]. Ensuring a sufficient supply of REEs is crucial to meet the growing demand. Therefore, ion adsorption clays are identified as a promising alternative source to fulfil the increasing need for REEs, rather than solely relying on conventional sources such as bastnasite, monazite, and xenotime.

Ion exchange leaching has become an effective method for the REE extraction, as the majority of REEs, about 60% to 90%, are found in the ionic phase within the clay [5]–[8]. During the extraction process, REE^{3+} ions adsorbed onto the clay surface exchange with cations in the salt solution, such as NH_4^+. Consequently, the released REE^{3+} ions enter the external solution and are collected as a leachate solution. Ensuring the maximum REE^{3+} ions concentration in the leachate solution is essential in ion exchange leaching, as it indicates the effectiveness of the extraction process. This presents the advantage of a simpler and more cost-effective recovery process, utilizing a salt solution as the leaching solution, with commonly employed solutions including ammonium sulfate ($(NH_4)_2SO_4$), magnesium sulphate ($MgSO_4$), and sodium chloride (NaCl) [9]–[12]. $MgSO_4$ exhibits significant potential in increasing REE leaching efficiency as demonstrated by K. Chen et al. [13]. Their findings revealed that employing a 0.23 M $MgSO_4$ leaching solution led to an improved REE leaching efficiency of 96.19% following the second stage leaching, surpassing the 93.87% achieved with a 0.23 M $(NH_4)_2SO_4$ solution. Additionally, $MgSO_4$ solution effectively reduces aluminum (Al), a primary impurity in leachate solutions, while maintaining comparable levels of REE leaching efficiency with $(NH_4)_2SO_4$ solution, as evidenced by studies conducted by Ran et al. [12], Y. F. Xiao et al. [14], and Yanfei et al.[15].

Current research is primarily focused on conducting ion exchange leaching experiments to identify the best leaching solutions and optimum conditions for improving the efficiency of REE extraction[5], [11], [16], [17]. However, it's crucial to understand the leaching mechanism to achieve high efficiency with low cost and minimal environmental impact. Various factors affecting REE extraction from ion adsorption clays have been studied experimentally, including leaching solution type and concentration, temperature, pH, and time [13], [16], [18], [19]. Given the complexity of the process and the limitations of experimental work, modelling and simulation methods offer a promising approach to understand ion

***CORRESPONDING AUTHOR | N. Harun** | ✉ noorlisa@umpsa.edu.my

exchange leaching mechanisms for REE extraction [20]. Integrating modelling into the process can help reduce errors and optimize leaching conditions before real experiments, making the approach more efficient and cost-effective.

This paper aims to develop a mathematical model to represent the leaching process for recovering rare earth from ion adsorption clay. Existing models, such as Fick's Law and the Kerr Model, are limited in capturing the entire leaching reaction mechanism which include both diffusion and chemical reaction steps. Fick's Law explains the diffusion of REE ions and leaching solution cations under a concentration gradient, while the Kerr Model focuses on the ion exchange reaction between REE ions and leaching solution cations on the clay surface [21]. To address this gap, this study employs the Shrinking Core Model, selected for its ability to represent the full kinetic mechanism, including external diffusion, internal diffusion, and chemical reaction control steps [11], [12], [14], [22], [23]. The exploration of kinetics is essential due to the significant increase in REE leaching efficiency observed over time during the ion exchange reaction. In this study, magnesium sulphate ($MgSO_4$) was selected as the leaching solution, and ultimately, a mathematical equation will be formulated to predict REE leaching efficiency under specific leaching durations and conditions.

2. RESEARCH METHOD

In this study, the derivation of the three controlling steps - external, internal, and chemical reaction control was performed based on the first principal model. The rate determining step was identified among the three controlling steps, followed by the determination of rate constant and reaction order. Then, the model was used to determine the REE leaching efficiency parameter (α) using Microsoft Excel, where it was validated, and the REE leaching profile was subsequently analyzed. Figure 1 presents the process flow chart to develop the model equation for the reaction.

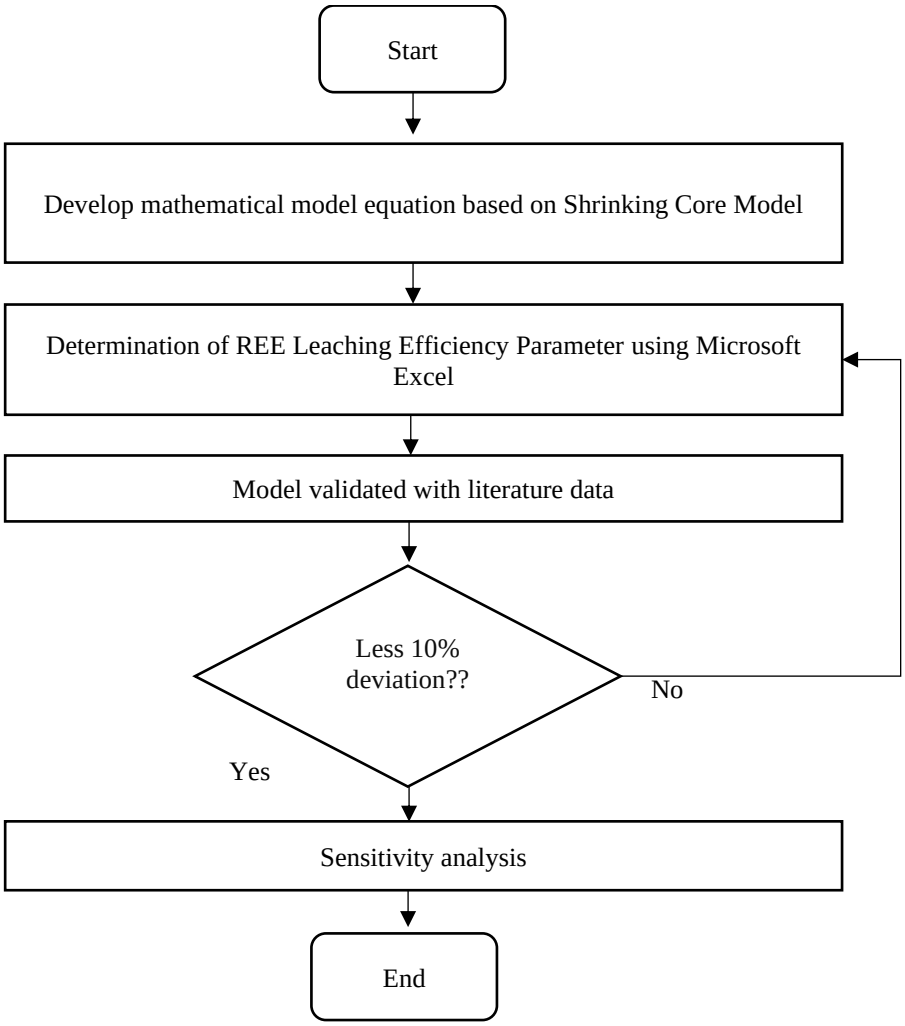

Figure 1. Process flow chart in development model equation for ion exchange leaching

2.1 Derivation Based on the First Principal Model

According to the Shrinking Core Model, the clay particle size remained constant throughout out the reaction with a significant number of impurities that remained as non-flaking ash or formed firm product materials as illustrated in Figure 2 [24], [25]. The outer layer of the clay particle was where the reaction takes place in this model. The reaction zone then penetrated the solid, creating fully converted material and inert solid, also known as ash. Thus, there was a core of unreacted material that remained at any time and shrank in size as the reaction continued, as demonstrated in Figure 3.

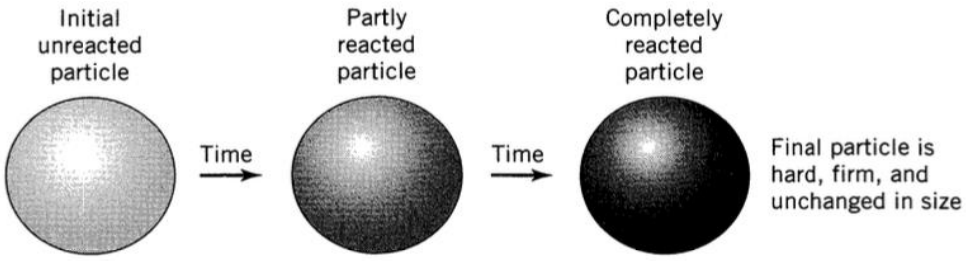

Figure 2. Process flow chart in development model equation for ion exchange leaching [25]

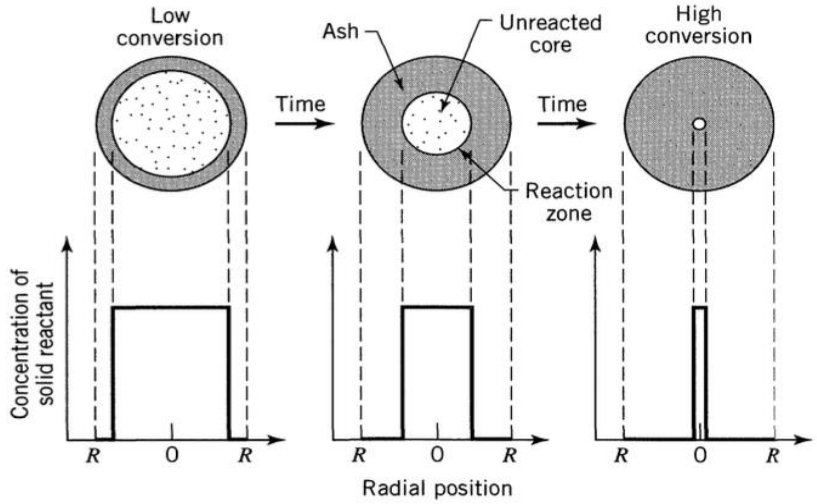

Figure 3. The unreacted core of the material shrank in size as the reaction continued Levenspiel [25]

The derivation of the Shrinking Core Model from the first principal model was referred to Levenspiel [25]. When formulating its kinetic equation, consideration was given to the thin liquid layer surrounding the clay particle's surface, which was considered as a liquid film. The ion exchange leaching reaction was described by Eq. **Error! Reference source not found.**, where A denoted the leaching solution, B represented the ionic phase of REEs in the ion adsorption clay, and b indicated the stoichiometry of reactant B. The resulting solid product represented the cation attached to the clay, while the liquid product was the leachate solution containing REEs.

$$A\,(l) + bB(s) \rightarrow solid\ product + liquid\ product \quad (1)$$

2.2 Diffusion through Liquid Film Controls (External Diffusion)

Whenever the resistance of the liquid film was a controlling factor, the concentration profile of liquid reactant A was illustrated in Figure 4. From the figure, there was no liquid reactant presented at the particle surface, resulting in the concentration of liquid reactant at the particle surface, C_{AS} was zero. Thus, the driving force was simplified from $C_{Al} - C_{AS}$, to just C_{Al} which referred to the concentration of liquid reactant A, and it remained constant throughout the entire reaction. The focus was directed toward the constant exterior surface of a clay particle, S_{ex} since it was convenient to derive the kinetic equations based on the available surface. Notably, by recognizing the stoichiometry of Eq. **Error! Reference source not found.**, that $dN_B = bdN_A$, expressing the rate of change N_B in terms of N_A using that stoichiometry, introducing terms related constant exterior surface of a clay particle, S_{ex}, Eq. 1 was developed.

$$\frac{1}{S_{ex}}\frac{dN_B}{dt} = \frac{1}{4\pi R^2}\frac{dN_B}{dt} = \frac{b}{4\pi R^2}\frac{dN_A}{dt} = bk_g\,(C_{Al} - C_{As}) = bk_g\,C_{Al} = constant \quad (1)$$

where $S_{ex}$was the exterior surface area of a clay particle, N_B was the moles of REEs, N_A was the moles of the leaching solution, t was the leaching time, R was the radius of the clay particle, b was the stoichiometric of REEs, k_g was the mass transfer coefficient between fluid and particle, C_{Al} was the concentration of the leaching solution and C_{AS} was the leaching solution concentration at the particle surface.

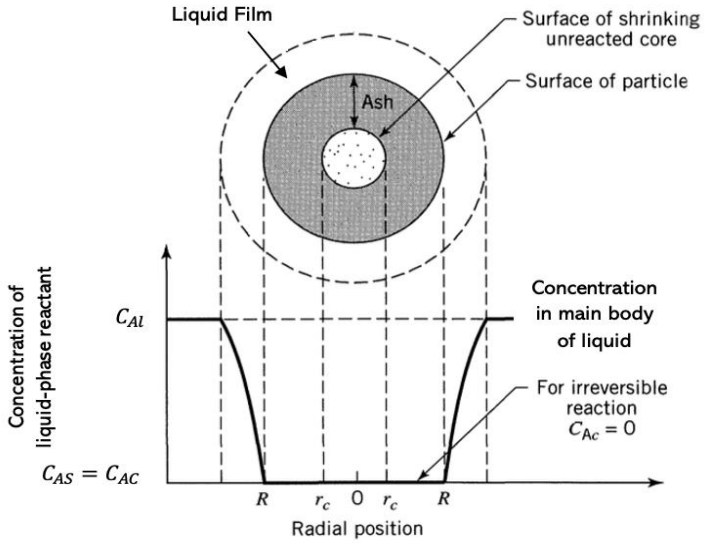

Figure 4. Representation of reacting particle when diffusion through liquid film was the controlling factor Levenspiel [25]

Letting ρ represent the molar density of B within the solid particle and V represent the particle's volume, the quantity of B presented in a solid particle was calculated by using Eq. 2.

$$N_b = \rho_B V = \left(\frac{moles\ B}{m^3 solid}\right)(m^3 solid) \tag{2}$$

The volume or radius of unreacted core reduction, r_c was corresponded to the disappearance of dN_B, therefore the moles of solid reactant B were expressed through Eq. 3.

$$-dN_B = -b\ dN_A = -\rho_B dV = -\rho_B d\left(\frac{4}{3}\pi r_c^3\right) = -4\pi\rho_B r_c^2 dr_c \tag{3}$$

Substituting Eq. 3 into Eq. 1, provided the reaction rate with respect to the unreacted core's shrinking radius, as shown in Eq. 4.

$$-\frac{1}{S_{ex}}\frac{dN_B}{dt} = -\frac{\rho_B r_c^2}{R^2}\frac{dr_c}{dt} = bk_g\ C_{Al} \tag{4}$$

Rearranging and integrating provided insight into how the radius of unreacted core shrinks with time as shown in Eq. 5.

$$\frac{\rho_B}{R^2}\int_R^{r_c} r_c^2 dr_c = bk_g\ C_{Al}\int_0^t dt$$

$$t = \frac{\rho_B R}{3bk_g\ C_{Al}}\left[1 - \left(\frac{r_c}{R}\right)^3\right] \tag{5}$$

Assuming the time required for total conversion of the particle was τ. Then substituted the value of $r_c = 0$ in Eq. 5, assuming that the unreacted core had already disappeared when the conversion was complete, resulting in the development of Eq. 6.

$$\tau = \frac{\rho_B R}{3bk_g\ C_{Al}} \tag{6}$$

The expression for the unreacted core's radius with respect to the time required for total conversion was derived by combining Eq. 5 and 6, resulting in Eq. 7.

$$\frac{t}{\tau} = 1 - \left(\frac{r_c}{R}\right)^3 \tag{7}$$

This could be written in terms of the fractional conversion of reactant B by using Eq. 8.

$$1 - X_B = \left(\frac{volume\ of\ unreacted\ core}{total\ volume\ of\ particle}\right) = \frac{\frac{4}{3}\pi r_c^3}{\frac{4}{3}\pi R^3} = \left(\frac{r_c}{R}\right)^3 \tag{8}$$

Therefore, the relationship of time with the radius of the unreacted core and the conversion of reactant B was explained by Eq. 9.

$$\frac{t}{\tau} = 1 - \left(\frac{r_c}{R}\right)^3 = 1 - (1 - X_B) = X_B \tag{9}$$

2.3 Diffusion through Ash Layer Controls (Internal Diffusion)

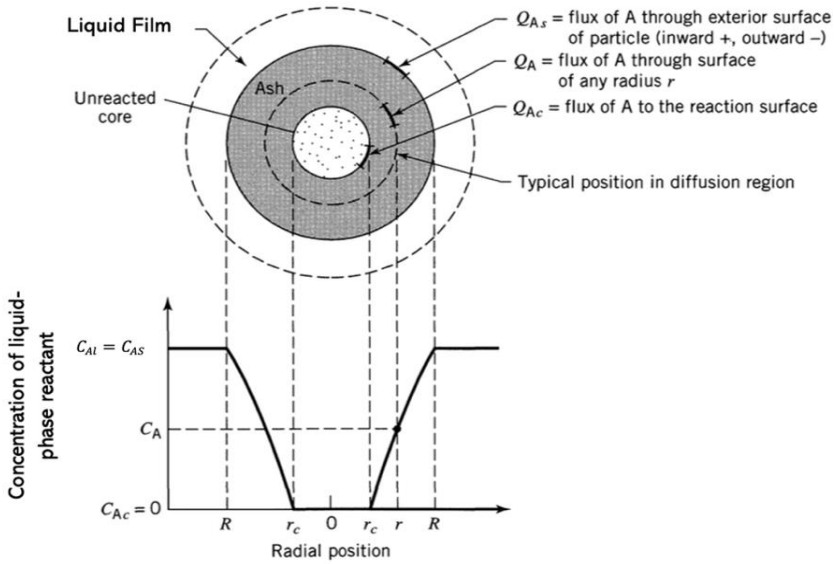

Figure 5 depicted a scenario where the controlling factor for the rate of reaction was the resistance of the diffusion through the ash. To establish a relationship between time and radius of unreacted core, like Eq. 5 for film resistance, a two-step analysis was necessary. Initially, examined a representative partially reacted particle and established the flux relationships under this condition. Subsequently, applied this relationship across all values of r_c, essentially integrating r_c, between R and 0.

By assuming the steady state condition, whereby the leaching system reached equilibrium, the rate of reaction of A at any instant was given by its rate of diffusion, Q to the reaction surface as depicted in Eq. 10 by referring to stoichiometric reaction in Eq. **Error! Reference source not found.**.

$$-\frac{dN_A}{dt} = 4\pi r^2 Q_A = 4\pi R^2 Q_{As} = 4\pi r_c^2 Q_{Ac} = \text{constant} \tag{10}$$

For simplicity, the flux of A through the ash layer was described using Fick's law for equal-molar counter diffusion. Eq. 11 was established by considering both Q_A and $\frac{dC_A}{dr}$ are positive values.

$$Q_A = \mathcal{D}_e \frac{dC_A}{dr} \tag{11}$$

The $\mathcal{D}_e$ is the effective diffusion of liquid reactant A in the ash layer. By combining Eq. 10 and 11, any value of r was obtained from Eq. 12.

$$-\frac{dN_A}{dt} = 4\pi r^2 \mathcal{D}_e \frac{dC_A}{dr} = constant \tag{12}$$

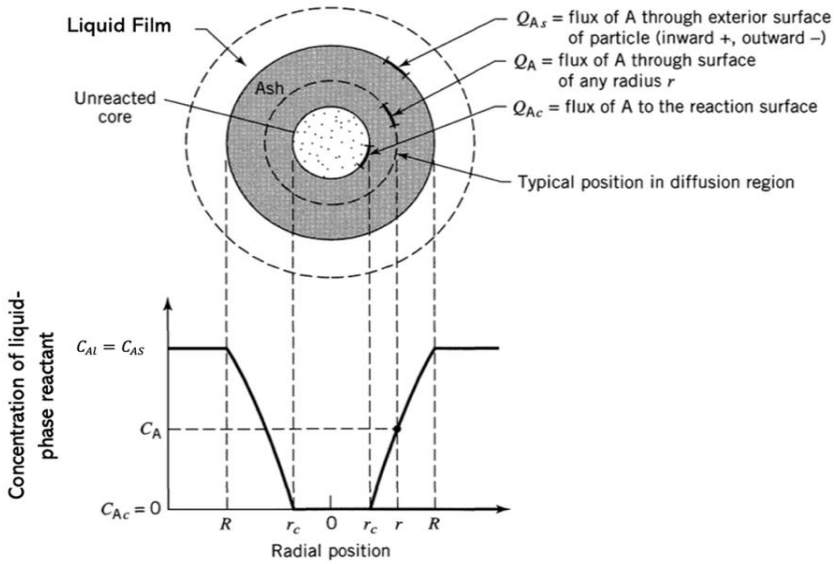

Figure 5. Representation of reacting particle when diffusion through ash is the controlling factor Levenspiel [25]

Calculating across the ash layer from R to r_c, yielded the following Eq. 13. This equation describes the state of a reacting particle at any point in time.

$$-\frac{dN_A}{dt}\int_R^{r_c}\frac{dr}{r^2} = 4\pi\mathcal{D}_e\int_{C_{Al}=C_{As}}^{C_{Ac}=0} dC_A$$

$$-\frac{dN_A}{dt}\left(\frac{1}{r_c}-\frac{1}{R}\right) = 4\pi\mathcal{D}_e C_{Al} \tag{13}$$

The variation in size of the unreacted core as time progressed was considered. For a given unreacted core's size, $\frac{dN_A}{dt}$ was constant; however, as the core shrank, the ash layer became thicker, leading to a reduction in the rate of diffusion of A. Hence, before proceeding with the integration of Eq. 13 which involved three variables, t, N_A, and r_c, it was necessary to eliminate one of these variables. Like film diffusion, N_A was eliminated by expressing it in terms of r_c. This relationship was represented by Eq. 3, hence, replacing it with Eq. 13., followed by the separation variables and integration, Eq. 14 was derived.

$$-\rho_B\int_{r_c=R}^{r_c}\left(\frac{1}{r_c}-\frac{1}{R}\right)r_c^2 dr_c = b\mathcal{D}_e C_{Al}\int_0^t dt$$

$$t = \frac{\rho_B R^2}{6b\mathcal{D}_e C_{Al}}\left[1-3\left(\frac{r_c}{R}\right)^2+2\left(\frac{r_c}{R}\right)^3\right] \tag{14}$$

For complete conversion of a particle, r_c was equal to 0 and the corresponding time required was expressed in Eq. 15.

$$\tau = \frac{\rho_B R^2}{6b\mathcal{D}_e C_{Al}} \tag{15}$$

The reaction's progress with respect to the time required for complete conversion was determined by combining Eq. 14 and Eq. 15, resulting in the formulation of Eq. 16.

$$\frac{t}{\tau} = 1-3\left(\frac{r_c}{R}\right)^2+2\left(\frac{r_c}{R}\right)^3 \tag{16}$$

When considering fractional conversion, as depicted in Eq. 8, Eq. 16 was transformed into Eq. 17.

$$\frac{t}{\tau} = 1-3(1-X_B)^{2/3}+2(1-X_B)$$

$$\frac{t}{\tau} = 1-\frac{2}{3}X_B-(1-X_B)^{2/3} \tag{17}$$

2.4 Chemical Reaction Controls

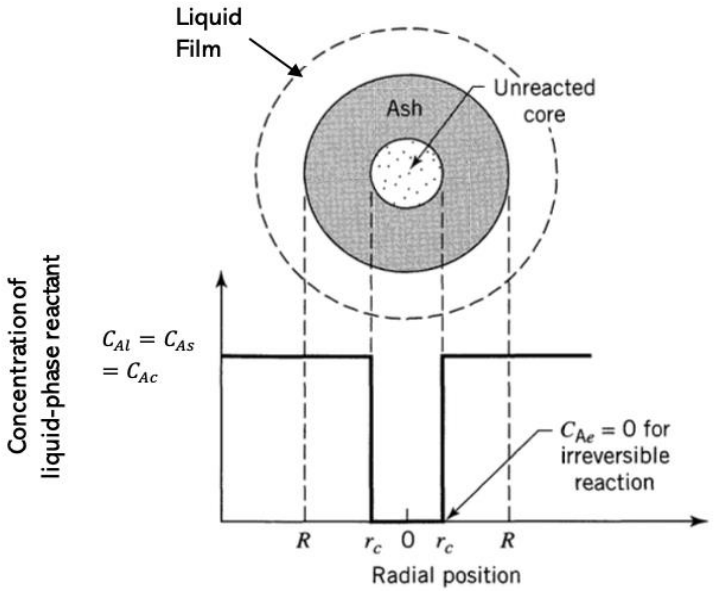

Figure 6 provided a visual representation of the concentration profiles inside a particle when chemical reactions were the controlling factor. Importantly, the chemical reaction's progress was independent of the existence of any ash layer, thus the reaction rate was proportional to the unreacted core's available surface. Eq. 18 was formulated using the reaction rate associated with the stoichiometry of Eq. **Error! Reference source not found.** according to the unreacted core surface area, r_c.

$$-\frac{1}{4\pi r_c^2}\frac{dN_B}{dt} = -\frac{b}{4\pi r_c^2}\frac{dN_A}{dt} = bk"C_{Al} \tag{18}$$

where k" was the first-order rate constant for the surface reaction. Expressing N_B in with respect to the shrinking radius of the unreacted core as demonstrated in Eq. 3 led to the formulation of Eq. 19.

$$-\frac{1}{4\pi r_c^2}\,\rho_B 4\pi r_c^2\frac{dr_c}{dt} = -\rho_B\frac{dr_c}{dt} = bk"C_{Al} \tag{19}$$

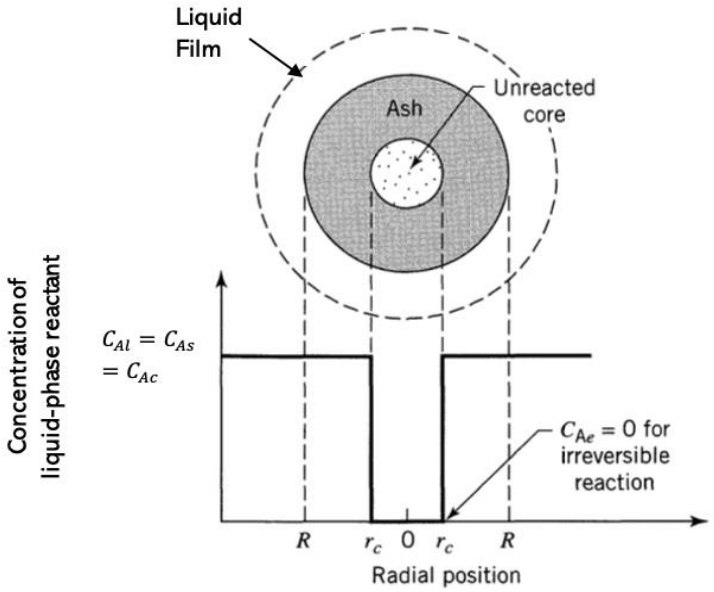

Figure 6. Representation of reacting particle when the chemical reaction is the controlling factor Levenspiel [25]

Table 1. Conversion-time equation based on the Shrinking Core Model

Controlling Factor			Time-Conversion Equation	
Liquid Film (External Diffusion)			$\frac{t}{\tau} = X_B$	9
	t	=	reaction time	
	τ	=	time for complete conversion	
	X_B	=	fractional conversion of REEs	
			$\tau = \frac{\rho_B R}{3bk_g\, C_{Al}}$	6
	ρ_B	=	molar density of REEs in the clay particle	
	R	=	radius of the clay particle	
	b	=	stoichiometric reaction of REEs	
	k_g	=	mass transfer coefficient	
	C_{Al}	=	concentration of leaching solution	
	Equation used:			20
			$\alpha = kt$	
	α	=	REE Leaching efficiencies (X_B)	
	k	=	Rate constant ($\frac{1}{\tau} = \frac{3bk_g\, C_{Al}}{\rho_B R}$)	
	t	=	reaction time	
Ash Layer Control (Internal Diffusion)			$\frac{t}{\tau} = 1 - \frac{2}{3}X_B - (1 - X_B)^{2/3}$	17
	t	=	reaction time	
	τ	=	time for complete conversion	
	X_B	=	fractional conversion of REEs	
			$\tau = \frac{\rho_B R^2}{6b\mathcal{D}_e C_{Al}}$	15
	ρ_B	=	molar density of REEs in the clay particle	
	R	=	radius of the clay particle	
	b	=	stoichiometric reaction of REEs	
	$\mathcal{D}_e$	=	diffusion coefficient of leaching solution in the ash layer	
	C_{Al}	=	concentration of leaching solution	
	Equation used:			21
			$1 - \frac{2}{3}\alpha - (1 - \alpha)^{2/3} = kt$	
	α	=	REE Leaching efficiencies (X_B)	
	k	=	Rate constant ($\frac{1}{\tau} = \frac{6b\mathcal{D}_e C_{Al}}{\rho_B R^2}$)	
	t	=	reaction time	
Chemical reaction			$\frac{t}{\tau} = 1 - (1 - X_B)^{1/3}$	25
	t	=	reaction time	
	τ	=	time for complete conversion	
	X_B	=	fractional conversion of REEs	
			$\tau = \frac{\rho_B R}{bk" C_{Al}}$	24
	ρ_B	=	molar density of REEs in the clay particle	
	R	=	radius of the clay particle	
	b	=	stoichiometric reaction of REEs	
	$k"$	=	first-order rate constant	
	C_{Al}	=	concentration of leaching solution	
	Equation used:			22
			$1 - (1 - \alpha)^{1/3} = kt$	
	α	=	REE Leaching efficiencies (X_B)	
	k	=	Rate constant ($\frac{1}{\tau} = \frac{bk" C_{Al}}{\rho_B R}$)	
	t	=	reaction time	

Performing integration resulted in the formulation of Eq. 23.

$$-\rho_B \int_R^{r_c} dr_c = bk"C_{Al} \int_0^t dt$$
$$t = \frac{\rho_B}{bk"C_{Al}}(R - r_c) \quad (23)$$

The required time, τ for total conversion was obtained when $r_c = 0$ was presented in Eq. 24.

$$\tau = \frac{\rho_B R}{bk"C_{Al}} \quad (24)$$

The decreased radius of the particle and increase in fractional conversion in terms of the time required for complete conversion was found by combining Eq. 23 and Eq. 24, resulting in the formulation of Eq. 25.

$$\frac{t}{\tau} = 1 - \frac{r_c}{R} = 1 - (1 - X_B)^{1/3} \quad (25)$$

Table 1 summarizes the conversion-time expression for sphere particles which is represented by the ion adsorption clay based on the Shrinking Core Model. The final equations used in this study were summarized in Eq. 20 for external diffusion control, Eq. 21 for internal diffusion control, and Eq. 22 for chemical reaction control.

2.5 Determination of Rate-Determining Step

The rate-determining step was the slowest part of the chemical reaction, which controlled the speed (rate) at which the overall reaction occurred. To proceed with this step, the experimental data on REE leaching efficiency, α represented by a versus time at varying $MgSO_4$ solution concentration, was taken from the study conducted by Ran et al. [12] shown in Figure 7.It was important to note that the experimental data obtained was conducted by using column leaching experiments, which effectively represented an in-situ leaching method. From that experiment, 250 grams of ore, consisting of 50% clay with particle size greater than 0.5mm was utilized, applying a liquid-to-solid ratio of 1.2:1 for the $MgSO_4$ solution to the solid clay. The leaching solution was introduced at a flow rate of 0.5 mL per minute, maintaining a pH level of 5.6, and the experiment was conducted at room temperature.

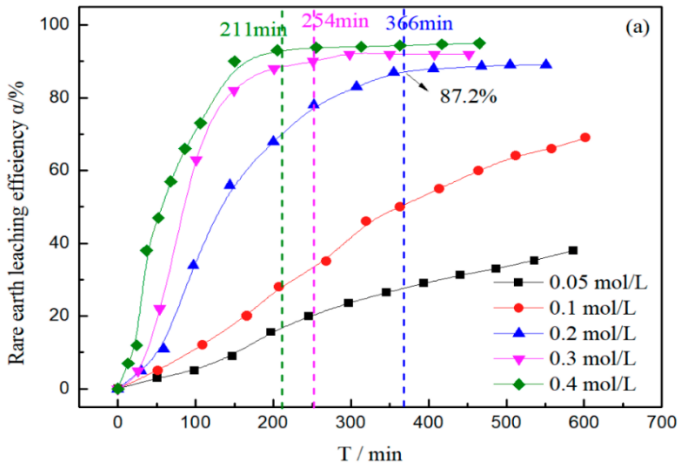

Figure 7. Graph of leaching efficiencies of REEs (α) versus time at different concentrations of $MgSO_4$ solution [12]

From Figure 7 , it was observed that the leaching process was categorized into three phases. The first phase was categorized as a slow and unstable process. Subsequently, the second phase, marked by fast and stable, exhibited a rapid increase in the leaching rate of REEs. Finally, the third phase represented the equilibrium stages in which REE leaching efficiency reached optimum level. Clearly, the key step of the reaction was the second stage. Therefore, the data of this stage was selected and substituted into these three kinetic control models. The graph of REE leaching efficiency, α versus time, t was plotted for internal diffusion, $1-\frac{2}{3}\alpha\ -(1-\alpha)^{2/3}$ versus t for external diffusion and $1-(1-\alpha)^{1/3}$ versus t for chemical reaction [11], [22], [26]. The rate-determining step among the three controlling steps would be identified as the one showing a straight linear relationship characterized by the greatest coefficient of determination, R^2, and the lowest slope value. The kinetic equation that represents the rate-determining step will be employed in the next step in determining rate constant.

2.6 Determination of Rate Constant (k) and Reaction Order (n)

To establish a mathematical model equation, it was essential to determine the rate constant, k. Typically, the rate constant, k was derived from the first principal model and was often expressed in terms of the time required for complete conversion, τ. However, obtaining the necessary data from literature reviews to calculate k might be challenging. Therefore, an alternative approach was proposed, wherein a semi-empirical equation was employed to estimate the rate constant, k. In this method, experimental data from Ran et al. [12] was utilized, and the rate constant, k was determined by applying the formula in Eq. 26.

$$k = k_o(C_A)^n \tag{26}$$

where k_o was the apparent rate constant, C_A was the leaching solution concentration and n was the reaction order. To find the k_o and n, Eq. 26 was expanded by taking the natural logarithm on both sides which resulted in the formulation of Eq. 27. From that formula, a graph of $ln\,k$ versus $ln\,(C_A)$ was plotted. The value of n was represented by the slope of the graph while the value of k_o was represented by the y-intercept of the graph.

$$lnk = n\,ln(C_A) + lnk_o \tag{27}$$

2.7 Determination of REE Leaching Efficiency Parameter (α)

To solve the developed equation model, an iterative numerical method was utilized. This method was implemented using the Goal Seek tool in Microsoft Excel to obtain the solution as shown in Figure 8. Specifically, it employed an iterative numerical algorithm to adjust the input value iteratively until the desired target value was approximately obtained

in the specified output cell. The input of leaching time, t, and the concentration of the leaching solution, C_A was defined, and the output of REE leaching efficiency, α was calculated.

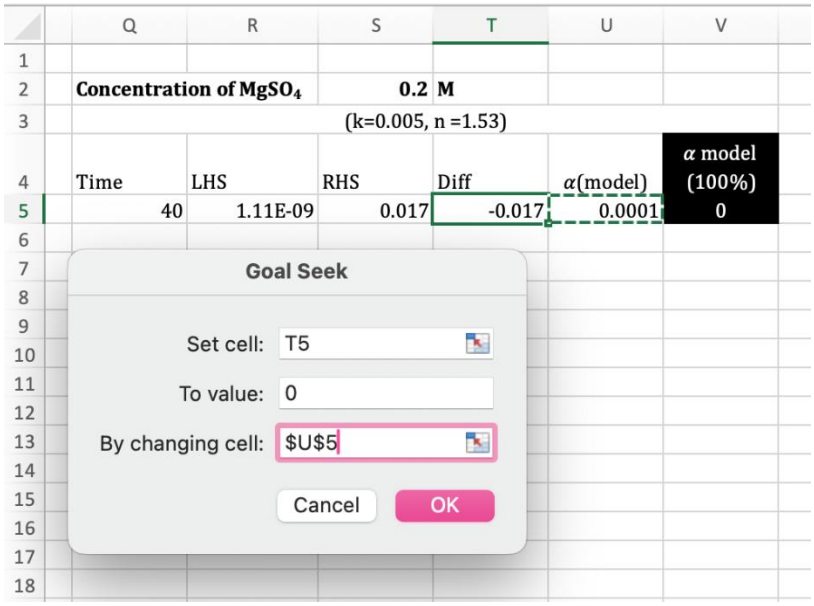

Figure 8. Determination of REE leaching efficiency using iterative goal seek method in Microsoft Excel

2.8 Model Validation

The agreement between observed and simulated data of REE leaching efficiency over time at different concentrations of $MgSO_4$ solution was analyzed by using statistical measures introduced by Willmott, consisting of index of agreement, d, root mean squared error (RMSE), and normalized root mean square error (NRMSE) [27]–[29]. The model validation process utilized the experimental data from Yanfei et al. [15]. In the conducted experiment, a quantity of 300 grams of ore, comprising clay particles with sizes ranging from 0.6 mm to 0.90 mm, was employed in the column leaching test. A leaching solution with a concentration of 0.2 M $MgSO_4$ was introduced at a flow rate of 0.6 mL per minute, with a constant pH of 5.7, and the experiment was carried out at a temperature of 298 K. There was a limitation in the experimental data available for model validation, specifically, the data employing $MgSO_4$ as the leaching solution for the leaching experiment using column. The experimental data from Yanfei et al. [15] was identified as the most suitable since the leaching condition applied almost the same as the leaching condition in the experiment by Ran et al. (2017), which was used for model formulation for obtaining the value of k and n.

The index of agreement, d was a measure of the degree of how close the simulated data, S_i aligned with the observed data, O_i that was obtained from the experimental result. The resulting value of d was obtained within the range of 0 to 1 where a value approaching 1 signified a high degree of agreement, while a value approaching 0 indicated a lack of agreement [30] When dealing with a collection of n paired data points, the calculation of d followed the formula outlined by Eq. 28 [28], [31], [32].

$$d = 1 - \frac{\sum_{i=1}^{n}(S_i - O_i)^2}{\sum_{i=1}^{n}(|S_i - \bar{O}| + |O_i - \bar{O}|)^2} \tag{28}$$

where $\bar{O}$ was the mean value of O_i. According to Liu et al. [32], the model classification criteria were as follows: "excellent" model agreement for $d \geq 0.9$, "good" model agreement for $0.8 \leq d < 0.9$, "moderate" model agreement for $0.7 \leq d < 0.8$, and "poor" model agreement for $d < 0.7$.

In addition, RMSE was the measure of overall accuracy of the model prediction which calculated the sum of the differences between simulated and observed data. RMSE was expressed in the same units as the dataset. The formula of RMSE was calculated by using Eq. 29 [31]–[33].

$$RMSE = \sqrt{\frac{\sum_{i}^{n}(S_i - O_i)^2}{n}} \tag{29}$$

where n was the number of observations. A lower RMSE indicated that the developed model was more effective in minimizing the differences between observed and simulated data, suggesting a closer fit between the model's predictions and the actual measurements.

Even though RMSE was widely as an overall indicator of model performance, it was sensitive to the impact of extreme values and failed to differentiate whether the model was overestimating or underestimating. Consequently, it was recommended to incorporate the normalized root mean square error (NRMSE) into the evaluation of the model

performance. NRMSE was calculated by dividing the RMSE value by either the mean of the observed data or the range of the observed data, depending on the nature of the experimental dataset. In this case, where REE leaching efficiency, α, increased from 0 to 1 with an extended leaching time, the range of the observed data was selected for the calculation of NRMSE, as shown in Eq. 30 [34].

$$Normalized\ RMSE\ (NRMSE) = \frac{RMSE}{y_{max-}y_{min}} x\ 100\% \quad (30)$$

where y_{max} was the maximum value of the observed data and y_{min} was the minimum value of the observed data. This normalization was important as it allowed for comparison of the RMSE across different datasets. NRMSE was expressed in a percentage and served as an indicator of the relative error difference between the simulation data computed by the model and the observed data collected through the experiment. According to Jamieson et al. [35], the model classification criteria were as follows: "excellent" for NRMSE < 10%, "good" for 10%<NRMSE<20%, "satisfactory" for 20%<NRMSE<30%, and "unsatisfactory" for NRMSE > 30%.

2.9 REE Leaching Profile Analysis

In REE leaching profile analysis, a comprehensive exploration and discussion were conducted to assess how variations in the leaching solution concentration and leaching time impacted the behaviour of REE leaching efficiency, α by using the developed model. The REE leaching efficiency was assessed across concentrations of 0.1 M, 0.2 M, 0.3 M, 0.4 M, 0.5 M, and 0.6 M, with leaching durations ranging from 0 to 2000 minutes. This exploration potentially involved using graphical representations to illustrate these effects. The objective was to verify whether the mathematical model developed in this study accurately represents the real behaviour of the ion exchange leaching process.

3. RESULT AND DISCUSSION

3.1 Determination of Rate Determining Step

Figure 9, Figure 10, and Figure 11 depicted the fitting curve for these three-kinetics reaction control model across various concentrations of $MgSO_4$ solution, respectively.

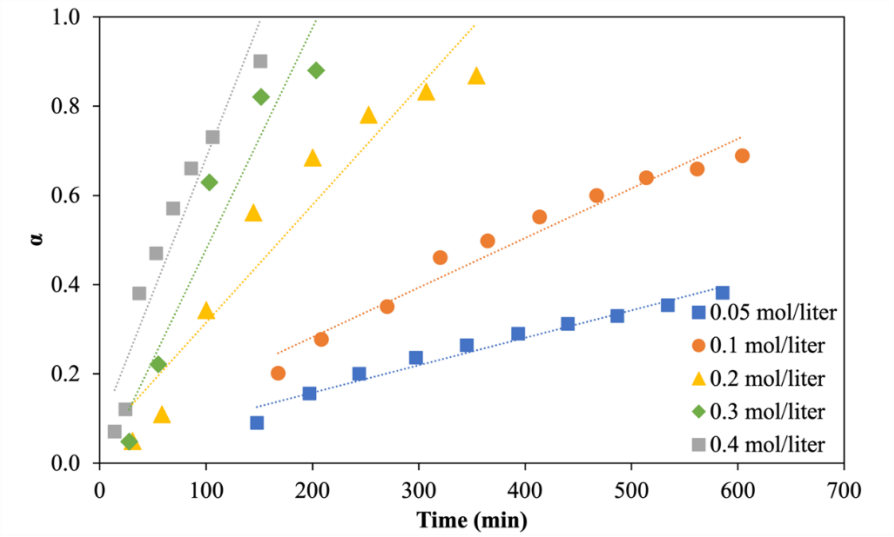

Figure 9. The fitted curve of external diffusion control model over time

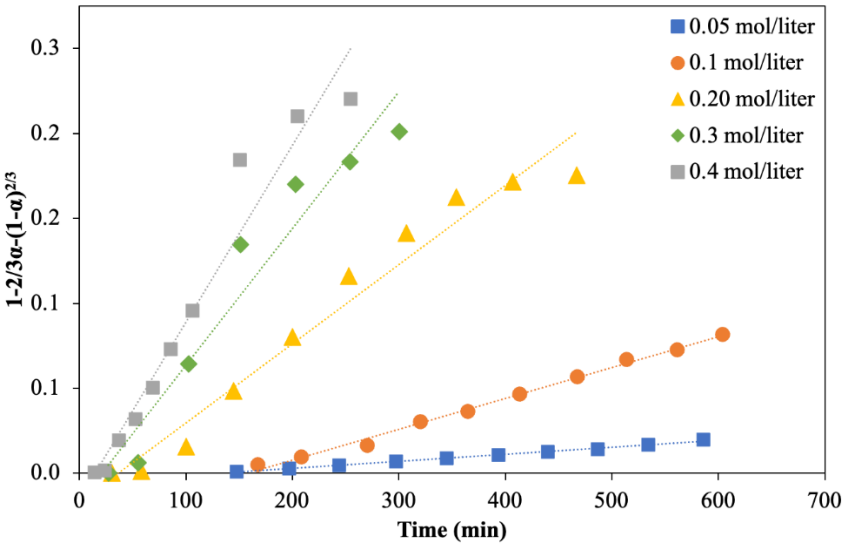

Figure 10. The fitted curve of internal diffusion control model over time

The apparent rate constant, k which was obtained from the slope value and correlation coefficient value, R^2 at different concentrations of MgSO4 solution for each kinetic model of external diffusion, internal diffusion, and chemical reaction, were presented in Table 2. The result revealed that the internal diffusion control model, as indicated by the plot of $1 - \frac{2}{3}\alpha - (1-\alpha)^{2/3}$ versus t, exhibited the most favourable linear relationship compared to the external and chemical reaction control models. This observation was supported by the lowest value of k and highest the value of R^2 obtained across all concentrations of $MgSO_4$ solution for the internal diffusion control model when compared to the external and chemical reaction control models.

The rate constant, k represented the speed of the reaction. A lower value of k suggested that the reaction was slower under the internal diffusion control model compared to the other two models. Meanwhile, R^2 measured how well the experimental data fit the model. In this context, the highest R^2 value meant that the internal control model provided the best fit for experimental data among the three models. As a result, it could be concluded that the internal diffusion control model played the role of the rate-determining step governing the leaching reaction. This finding of the internal diffusion control model as the rate-determining step was in the same agreement with the finding of studies conducted by Chai et al. [11], L. Zhang et al.[36], Jun et al. [22], Ran et al. [12], Tian et al. [23], and Y. F. Xiao et al. [14].

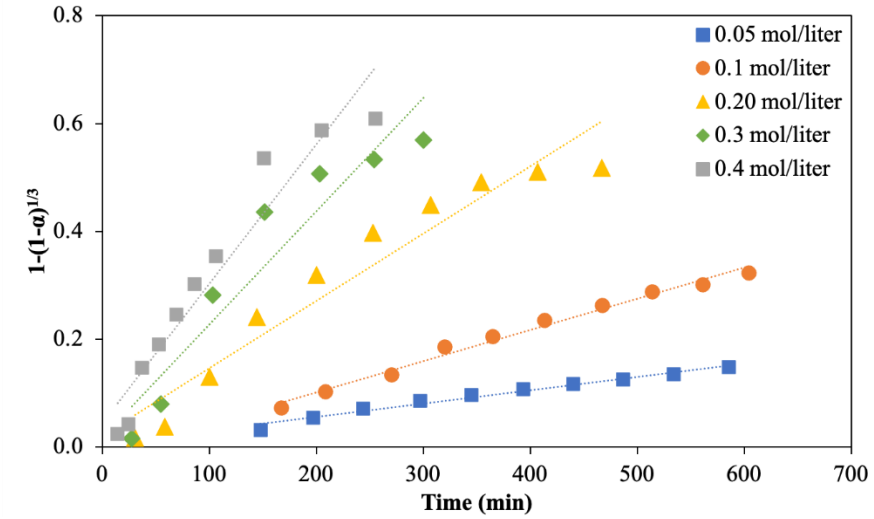

Figure 11. The fitted curve of chemical reaction control model over time

Theoretically, internal diffusion was determined as the rate-determining step primarily due to the complex and porous layer of the clay minerals. This layer created significant barriers to the movement of ions within it, causing the process of internal diffusion to occur slowly. Consequently, the rate at which ions could penetrate through this porous layer became the limiting factor in the overall leaching process. On the other hand, external diffusion, which included the transfer of ions from the leaching solution to the clay surface through the liquid film, occurred quite quickly since ions could move freely within the liquid phase. In contrast, the chemical reaction itself, where the cations exchanged with REE ions on the available surface of the unreacted core, tended to occur rapidly at active sites.

Table 2. The apparent rate constant, $\boldsymbol{k}$ and correlation coefficient, $\boldsymbol{R^2}$, value for external, internal, and chemical reaction control model

Concentration of $MgSO_4$ solution, (M)	External Diffusion Control Model		Internal Diffusion Control Model		Chemical Reaction Control Model	
	R^2	Slope, K (min^{-1})	R^2	Slope, K (min^{-1})	R^2	Slope, K (min^{-1})
0.05	0.9657	0.0006	0.9966	0.00004	0.9778	0.0002
0.1	0.9634	0.0011	0.9946	0.0002	0.9866	0.0006
0.2	0.9144	0.0026	0.965	0.0005	0.9314	0.0012
0.3	0.9188	0.005	0.9419	0.0008	0.9042	0.0021
0.4	0.9177	0.0061	0.9539	0.001	0.9282	0.0026

3.2 Determination of Rate Constant (k) and Reaction Order (n)

In this step, the equation for internal diffusion control in Eq. 31 was employed as it governed the rate-determining step, effectively representing the overall leaching process. According to the original internal diffusion, the rate constant, k was obtained from Eq. 32.

$$1 - \frac{2}{3}\,\alpha - (1-\alpha)^{\frac{2}{3}} = kt \tag{31}$$

$$k = k_o(C_{Mg^{2+}})^n \tag{32}$$

where k_o was the apparent rate constant, $C_{Mg^{2+}}$ was the concentration of $MgSO_4$ solution, and n is the reaction order. The value of k_o and n could be determined from Eq. 33 by plotting the graph of the natural logarithm of k against $C_{Mg^{2+}}$ as illustrated in

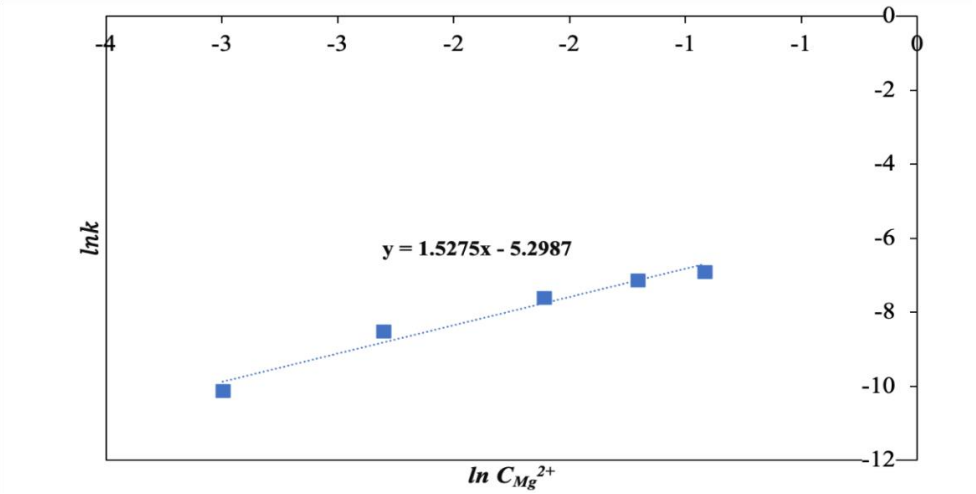

Figure 12. Notably to plot this graph, these k and $C_{Mg^{2+}}$ values corresponded to the internal diffusion control model were obtained from

Table 1.

$$lnk = n\ ln(C_{Mg^{2+}}) + lnk_o \tag{33}$$

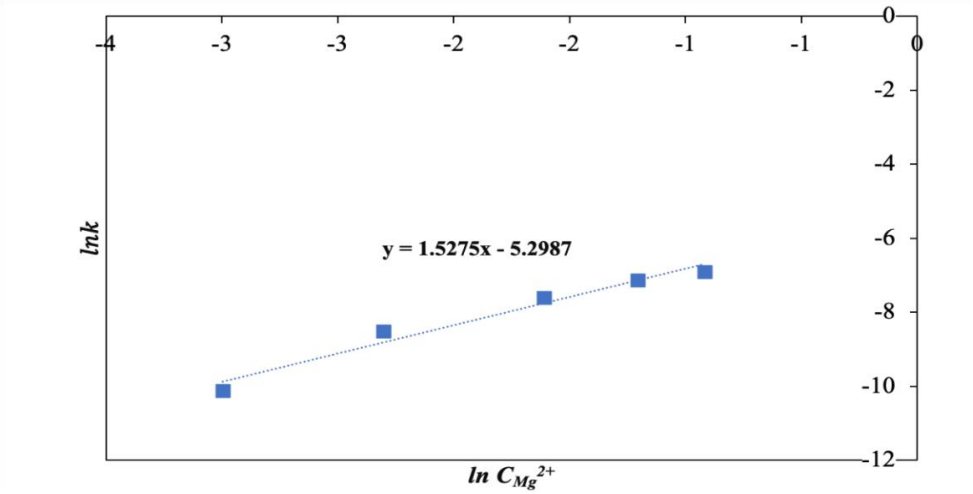

Figure 12. Relationship between lnk and $lnC_{Mg^{2+}}$

The value of reaction order, n was determined as the slope of the graph which was equal to 1.5275 while the value of the apparent rate constant, k_o was determined by the y-intercept of the graph, lnk_owhich was found to be -5.2987. Consequently, k_o was calculated to be 0.005. Therefore, the developed kinetic equation for the internal diffusion control model was represented by Eq. 34.

$$1 - \frac{2}{3}\alpha - (1-\alpha)^{\frac{2}{3}} = 0.005(C_{Mg^{2+}})^{1.53}t \tag{34}$$

3.3 Determination of REE Leaching Efficiency Parameter (α)

The REE leaching efficiency parameter (α) was determined across various concentrations of $MgSO_4$ solution using Eq. 34. Figure 13 illustrates an example of the REE leaching efficiency parameter (α) at a concentration of 0.2 M $MgSO_4$ over different time intervals.

	Q	R	S	T	U	V
1						
2	**Concentration of $MgSO_4$**		**0.2**	**M**		
3	(k=0.005, n =1.53)					
4	Time	LHS	RHS	Diff	α(model)	α model (100%)
5	40	1.70E-02	0.017	0.000	0.3564006	36
6	83	3.53E-02	0.035	0.000	0.4916696	49
7	124	5.19E-02	0.053	-0.001	0.577368	58
8	165	6.96E-02	0.070	-0.001	0.6485349	65
9	206	8.78E-02	0.088	0.000	0.707957	71
10	249	1.06E-01	0.106	0.000	0.7572092	76
11	291	1.25E-01	0.124	0.001	0.8001425	80
12	332	1.41E-01	0.142	0.000	0.8329261	83
13	375	1.60E-01	0.160	0.000	0.8642703	86
14	415	1.78E-01	0.177	0.001	0.8906345	89
15	456	1.94E-01	0.194	0.000	0.9120442	91
16	498	2.12E-01	0.212	0.000	0.9322053	93
17	540	2.30E-01	0.230	0.000	0.9490832	95
18	582	2.49E-01	0.248	0.001	0.9644761	96

Figure 13. Example of REE leaching efficiency results at 0.2 M of $MgSO_4$ solution

3.4 Model Validation

The model validation process utilized the experimental data from the study conducted by Yanfei et al. [15]. Figure 14 provided a comparison between the simulation and the experimental results for REE leaching efficiency, α. This

comparison was carried out across different time intervals at 0.2 M concentrations of $MgSO_4$ leaching solution, demonstrating a strong and consistent correlation between the two datasets. As time progressed, the leaching efficiencies of REEs exhibited an upward trend, reaching nearly maximum efficiency around the 500th minute.

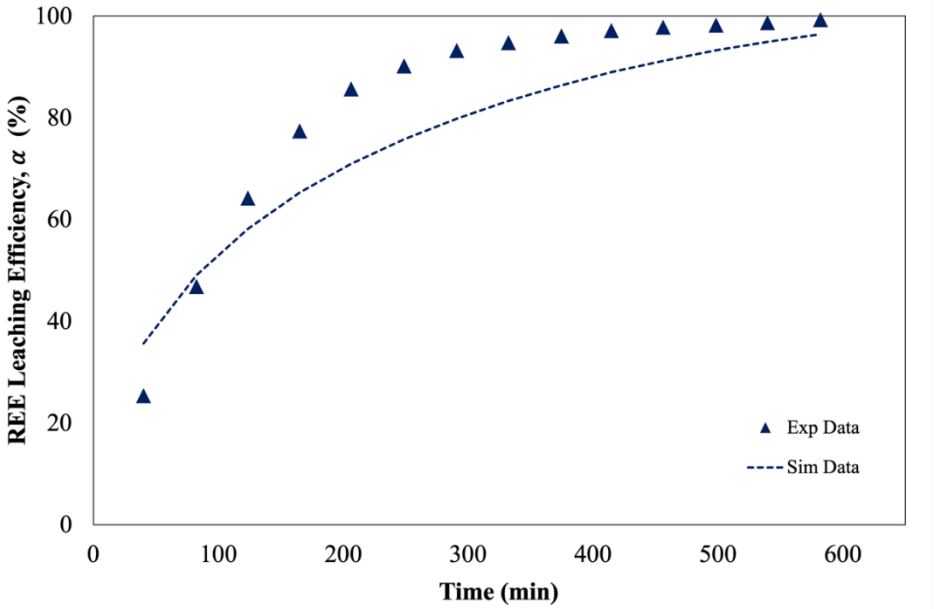

Figure 14. Simulations and experimental results for REE leaching efficiency over time at 0.2 M concentration of $MgSO_4$ solution

The statistical model validation for the index of agreement, d, and normalized root mean square error (NRMSE) are presented in Table 3. The statistical model validation results were favorable, as they showed a high value of d and a low value of NRMSE. The d values of 0.943 exceeded the 0.9 threshold, indicating excellent agreement with experimental data [32]. In terms of the NRMSE values, 12.98% of the values fell within the 10-20% range, indicating as good model performance [35]. However, as the model validation for NRMSE revealed deviations exceeding 10% in errors, modification was implemented to the model by fine-tuning the value of the reaction order, n to better align with the experimental data for the 0.2 M concentration of $MgSO_4$ solution.

Table 3. The statistical model validation at a 0.2 M concentration of $MgSO_4$ solution

Concentration of $MgSO_4$ solution (M)	Statistical Data	
	Index of agreement, d	NRMSE (%)
0.2	0.943	12.98

3.5 Modification of Reaction Order (n)

The modification of n was implemented by decreasing its value from 1.53 to 1.43, 1.33, 1.23 and 1.13. During this modification process, the value of the rate constant, k remained constant at 0.005. Figure 15 provided a visual comparison between simulation and the experimental results for REE leaching efficiency at concentration of 0.2 M $MgSO_4$ solution, corresponding to a different value of n. The statistical model validation results indicated that when the reaction order, n was set to 1.33, it led to the highest level of agreement, with a d value of 0.978, and the lowest NRMSE value, which was 7.9 %. The d value, close to 1, indicated a high degree of agreement how close the simulation data aligned with experimental data, while the low NRMSE value represented minimal relative error difference the two data sets. Table 4 displayed a summary of d and NRMSE values for different n values, highlighting that the optimal statistical performance occurred when n was set to 1.33.

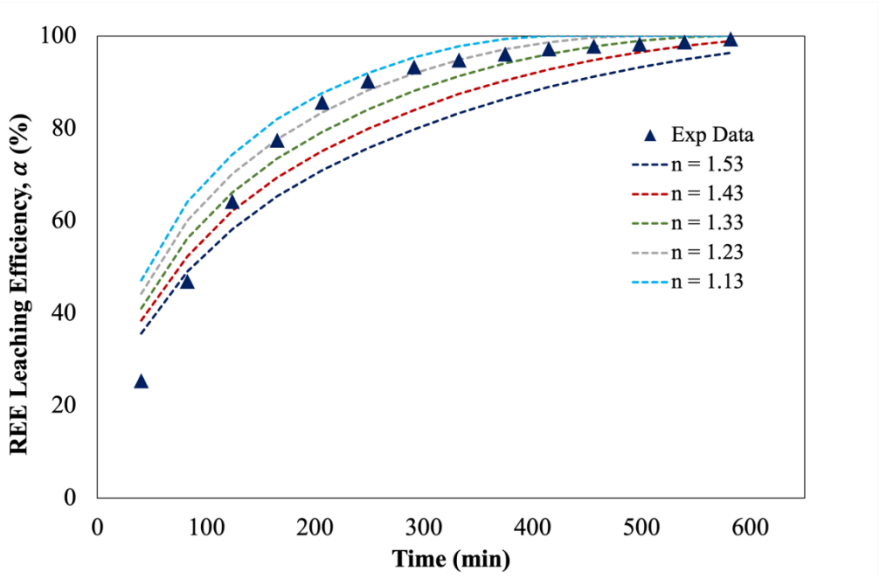

Figure 15. Comparison of the simulation and experimental data for REE leaching efficiency in 0.2 M $MgSO_4$ solution at different value of n

Table 4. The statistical model validation for different reaction order, n at 0.2 M $MgSO_4$ solution

Reaction order, n	Statistical Data	
	d	NRMSE (%)
1.53	0.943	12.98
1.43	0.968	9.53
1.33	0.978	7.90
1.23	0.972	8.77
1.13	0.953	11.08

Hence, the modified equation by using the new n value of 1.33 was presented in Eq. 35.

$$1-\frac{2}{3}\alpha-(1-\alpha)^{\frac{2}{3}}=0.005(C_{Mg^{2+}})^{1.33}t \tag{35}$$

Eq. 35 was simplified into Eq. 36.

$$\alpha=1-\sqrt{\frac{(0.005(C_{Mg^{2+}})^{1.33}t)-\frac{1}{3}}{(\frac{2}{3}\alpha-(1-\alpha)^{\frac{2}{3}})-1}}^{3} \tag{36}$$

3.6 Comparison of the Developed Model with Ran et al. [12] Model

The model developed in this study was compared with the model developed by Ran et al. [12] in terms of statistical model validation results. Both models employed the Shrinking Core Model with internal diffusion as the rate-determining step and employed $MgSO_4$ as the dedicated leaching solution. The process of model validation utilized the same experimental data from Yanfei et al. [15]. Figure 16 illustrates the results of REE leaching efficiency for both the developed model and the model developed by Ran et al. [12] at different time intervals using a 0.2 M concentration of $MgSO_4$ solution. The developed model exhibited a closer alignment with the experimental data compared to the model developed by Ran et al. [12]. This observation was further validated through the results of the statistical model validation. From Table 5, the developed model equation, in this study, indicated a higher value of d (0.978) and a lower value of NRMSE (7.90%) in contrast to the model equation developed by Ran et al. [12] (d = 0.967, NRMSE =9.77%), signifying an improvement in the performance of the developed model. In Figure 16, the REE leaching efficiency values predicted by the developed model in this study initially do not align well with the experimental data within the first 300 minutes. However, they begin to match more closely at 400 minutes and beyond. Nevertheless, the model consistently exhibits exponential growth in REE leaching efficiency, eventually reaching a maximum of 100% as leaching time progresses, mirroring the behavior observed in the experimental data. This demonstrates that the leaching behavior of REE extraction in this model follows the patterns observed in the leaching experiment. However, the model developed in this work was limited to conditions involving only $MgSO_4$ leaching solution, not applicable for others solution.

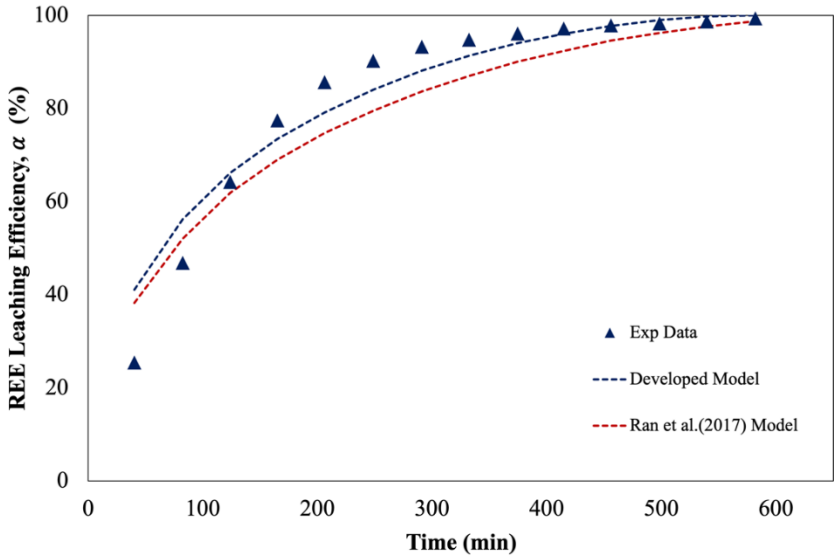

Figure 16. REE leaching efficiency for the developed model (this work) and the model developed by Ran et al. [12] at different time intervals using a 0.2 M concentration of $MgSO_4$ solution

Table 5. The statistical model validation for the developed model and the model developed by Ran et al. [12] at 0.2 M $MgSO_4$ solution

Model	Statistical Data	
	d	NRMSE (%)
Developed Equation $1-\frac{2}{3}\alpha-(1-\alpha)^{\frac{2}{3}}=0.005(C_{Mg^{2+}})^{1.33}t$	0.978	7.90
Ran et al. (2017) $1-\frac{2}{3}\alpha-(1-\alpha)^{\frac{2}{3}}=0.0075(C_{Mg^{2+}})^{1.69}t$	0.967	9.77

3.7 REE Leaching Profile Analysis

The relationship between REEs leaching efficiency over time at different concentrations of $MgSO_4$ leaching solution was described by Figure 17. The effect of the leaching time on REE leaching efficiencies was analyzed. As shown in Figure 17, the graph exhibited exponential growth in REE leaching efficiency, eventually approaching a maximum of 100% as the leaching time proceeded. As the time progressed, the REE leaching efficiency tended to increase gradually because the leaching solution gradually penetrates the clay ore, leading to an ion exchange reaction between REE ions and the cations in the leaching solution. However, there was a point at which REE leaching efficiency reached its maximum level and further extensions in the leaching time did not lead to any significant improvements in the leaching process. This occurred because the leaching process reached a state of equilibrium wherein all REE ions had undergone exchange with cations and subsequently dissolved into the leachate solution.

Regarding the effect of leaching solution concentration, it was observed that higher concentrations of the leaching solution tended to accelerate the leaching process, thus reducing the time required to reach the equilibrium and achieve maximum REE leaching efficiency. This occurred because higher concentrations of the leaching solution created a higher concentration gradient between the clay particles and the leaching solution. This concentration gradient acted as a driving force for mass transfer and facilitating the rapid transfer of REE ions from the clay particles into the leachate solution. As a result, the leaching process improved in efficiency, leading to a shorter duration for reaching equilibrium and achieving the maximum REE leaching efficiency.

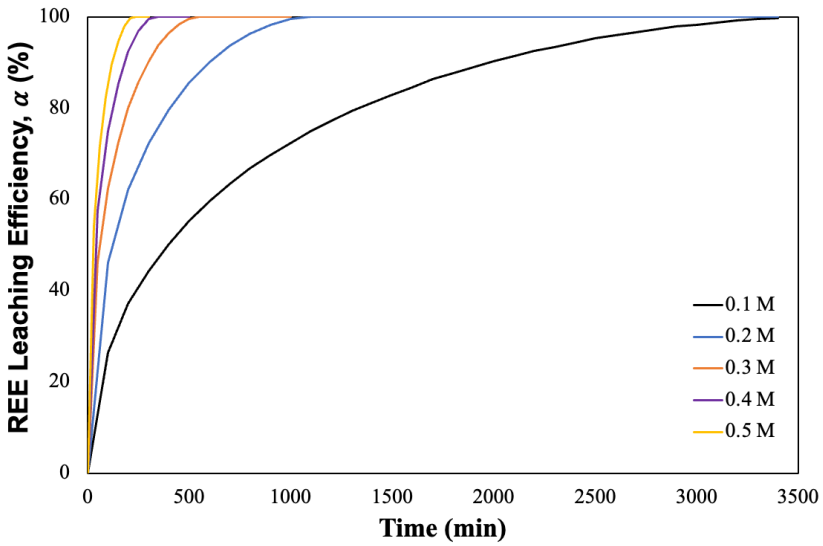

Figure 17. The relationship between REEs leaching efficiency and time at varying concentrations of $MgSO_4$ solution

4. CONCLUSION

In summary, this study has successfully formulated a mathematical model employing the Shrinking Core Model to represent the ion exchange leaching process for the extraction of REEs from ion adsorption clay. The investigation into the mechanism of ion exchange leaching during the formulation of the mathematical model involved determining the rate-determining step between internal diffusion, external diffusion, and chemical reaction. The results demonstrated that rate-determining step belonged to internal diffusion control which governed the overall leaching process, and its equation was used to develop the mathematical model. The formulated equation for this developed model was expressed as $1 - \frac{2}{3}\alpha - (1-\alpha)^{\frac{2}{3}} = 0.005(C_{Mg^{2+}})^{1.33}$. The statistical model validation demonstrated high level of agreement with the index value of d = 0.978, indicating an excellent agreement (d > 0.9) with experimental data and a low value of NRMSE = 7.90 %, indicating an excellent performance model (NRMSE < 10%). These values proved the model's efficiency in predicted REE leaching efficiency at different time across various concentration of $MgSO_4$ solution. The limitation of the developed model was constrained to conditions involving only $MgSO_4$ leaching solution, not applicable for others solution. This developed mathematical model holds significant promises for providing reliable data for industry stakeholders, government agencies, and policymakers. This, in turn, promises to advance the recovery of rara earth from ion adsorption clay and contribute to the industry's growth and sustainability.

ACKNOWLEDGEMENT

The authors acknowledge the financial support provided by the Ministry of Higher Education (MoHE) Malaysia under the Fundamental Research Grant Scheme (FRGS) No. FRGS/1/2021/TK0/UMP/02/26 (University reference RDU210130). The authors also extend their appreciation to Universiti Malaysia Pahang Al-Sultan Abdullah for the provision of laboratory facilities.

CONFLICT OF INTEREST

The authors declare that they have no known competing financial interests or personal relationships that could have appeared to influence the work reported in this paper.

AUTHORS CONTRIBUTION

N.A.M. Sobri was responsible for the methodology, software, validation, and investigation, while N. Harun contributed to the conceptualization and provided supervision.

REFERENCES

[1] A. Alshameri, X. Wei, H. Wang, Y. Fuguo, X. Chen, H. He, et al., "A review of the role of natural clay minerals as effective adsorbents and an alternative source of minerals," in *Minerals*, K. S. Essa, Ed., ch. 3, pp. 50-63, 2019.

[2] S. M. Jowitt, T. T. Werner, Z. Weng, and G. M. Mudd, "Recycling of the rare earth elements," *Current Opinion in Green and Sustainable Chemistry*, vol. 13, pp. 1–7, 2018.

[3] D. Yan, S. Ro, O. Sunam, and S. Kim, "On the global rare earth elements utilization and its supply-demand in the future," in *IOP Conf. Ser. Earth Environ. Sci.*, vol. 508, no. 1, p. 012084, 2020.

[4] R. Ganguli and D. R. Cook, "Rare earths: A review of the landscape," *MRS Energy & Sustainability*, vol. 5, no. 1, pp. 1–16, 2018.

[5] N. A. M. Sobri, N. Harun, and M. Y. M. Yunus, "A review of the ion exchange leaching method for extracting rare earth elements from ion adsorption clay," *Chemical Engineering Research and Design*, vol. 208, pp. 94-114, 2024.

[6] N. A. Sobri, M. Y. B. M. Yunus, and N. Harun, "A review of ion adsorption clay as a high potential source of rare earth minerals in Malaysia," *Materials Today: Proceedings*, 2023.

[7] J. Chen, J. Qiu, L. Huang, X. Chen, Y. Yang, and Y. Xiao, "Coordination–reduction leaching process of ion-adsorption type rare earth ore with ascorbic acid," *Journal of Rare Earths*, vol. 41, no. 8, pp. 1225–1233, 2023.

[8] G. Moldoveanu and V. Papangelakis, "An overview of rare-earth recovery by ion-exchange leaching from ion-adsorption clays of various origins," *Mineralogical Magazine*, vol. 80, no. 1, pp. 63–76, 2016.

[9] S. Peelman, Z. H. I. Sun, J. Sietsma, and Y. Yang, "Leaching of rare earth elements: Past and present," *Rare Earths Industry: Technological, Economic, and Environmental Implications*, pp. 446–456, 2014.

[10] S. Huang, J. Feng, Z. Ouyang, J. Yu, H. Hou, and R. Chi, "Dynamic elution of residual ammonium leaching agent from weathered crust elution-deposited rare earth tailings by magnesium chloride," *Environmental Research*, vol. 210, p. 112935, 2022.

[11] X. Chai, G. Li, Z. Chen, Z. Zhang, and R. Chi, "Leaching kinetics of weathered crust elution-deposited rare earth ore with compound ammonium carboxylate," *Minerals*, vol. 10, no. 6, p. 516, 2020.

[12] X. Ran, Z. Ren, H. Gao, R. Zheng, and J. Jin, "Kinetics of rare earth and aluminum leaching from kaolin," *Minerals*, vol. 7, no. 9, 2017.

[13] K. Chen, J. Pei, S. Yin, S. Li, J. Peng, and L. Zhang, "Leaching behaviour of rare earth elements from low-grade weathered crust elution-deposited rare earth ore using magnesium sulfate," *Clay Minerals*, vol. 53, no. 3, pp. 505–514, 2018.

[14] X. Huang and L. Huang, "Leaching characteristics of ion-adsorption type rare earths ore with magnesium sulfate," *Transactions of Nonferrous Metals Society of China*, vol. 25, no. 11, pp. 3784–3790, 2015.

[15] X. Yanfei, F. Zongyu, H. Xiaowei, H. Li, C. Yingying, W. Liangshi, et al., "Recovery of rare earths from weathered crust elution-deposited rare earth ore without ammonia-nitrogen pollution: I. leaching with magnesium sulfate," *Hydrometallurgy*, vol. 153, pp. 58–65, 2015.

[16] Q. Shi, Y Zhao, X Meng, L Shen, G Qiu, X Zhang, et al., "Column leaching of ion adsorption rare earth ore at low ammonium concentration," *Journal of Materials Research and Technology*, vol. 19, pp. 2135–2145, 2022.

[17] W. Nie, R. Zhang, Z. He, J. Zhou, M. Wu, Z. Xu, et al., "Research progress on leaching technology and theory of weathered crust elution-deposited rare earth ore," *Hydrometallurgy*, vol. 193, p. 105295, 2020.

[18] L. Yang, C. Li, D. Wang, F. Li, Y. Liu, X. Zhou, et al., "Leaching ion adsorption rare earth by aluminum sulfate for increasing efficiency and lowering the environmental impact," *Journal of Rare Earths*, vol. 37, no. 4, pp. 429–436, 2019.

[19] Z. Zhang, R. Chi, Z. Chen, and W. Chen, "Effects of ion characteristics on the leaching of weathered crust elution-deposited rare earth ore," *Frontiers in Chemistry*, vol. 8, pp. 1–14, 2020.

[20] P. Long, G. Wang, C. Zhang, Y. Huang, and S. Luo, "A two-parameter model for ion exchange process of ion-adsorption type rare earth ores," *Journal of Rare Earths*, vol. 38, no. 11, pp. 1251–1256, 2020.

[21] P. Long, G. Wang, C. Zhang, Y. Yang, X. Cao, and Z. Shi, "Kinetics model for leaching of ion-adsorption type rare earth ores," *Journal of Rare Earths*, vol. 38, no. 12, pp. 1354–1360, 2020.

[22] T. Jun, Y. Jingqun, C. Ruan, R. Guohua, J. Mintao, and O. Kexian, "Kinetics on leaching rare earth from the weathered crust elution-deposited rare earth ores with ammonium sulfate solution," *Hydrometallurgy*, vol. 101, pp. 166–170, 2010.

[23] J. Tian, R. Chi, and J. Yin, "Leaching process of rare earths from weathered crust elution-deposited rare earth ore," *Transactions of Nonferrous Metals Society of China*, vol. 20, no. 5, pp. 892–896, 2010.

[24] M. Y. Eisa, B. A. Abdulmajeed, and C. K. Hawee, "Kinetic study of the leaching of Iraqi Akashat phosphate ore using lactic acid," *Al-Khwarizmi Engineering Journal*, vol. 14, no. 1, pp. 128–135, 2018.

[25] O. Levenspiel, *Chemical Reaction Engineering*, 3rd Edition, John Wiley & Sons, 1999.

[26] F. Habashi, *Principles of Extractive Metallurgy*, vol. 1. CRC Press, 1969.

[27] D. R. Legates and G. J. McCabe Jr., "Evaluating the use of 'goodness-of-fit' Measures in hydrologic and hydroclimatic model validation," *Water Resources Research*, vol. 35, no. 1, pp. 233–241, 1999.

[28] C. J. Willmott, "Some comments on the evaluation of model performance," *Bulletin of the American Meteorological Society*, vol. 63, no. 11, pp. 1309–1313, 1982.

[29] C. J. Willmott, "On the validation of models," *Physical Geography*, vol. 2, no. 2, pp. 184–194, 1981.

[30] S. M. Robeson and D. G. Steyn, "Evaluation and comparison of statistical forecast models for daily maximum ozone concentrations," *Atmospheric Environment. Part B. Urban Atmosphere*, vol. 24, no. 2, pp. 303–312, 1990.

[31] U. Akumaga, A. Tarhule, and A. A. Yusuf, "Validation and testing of the FAO AquaCrop model under different levels of nitrogen fertilizer on rainfed maize in Nigeria, West Africa," *Agricultural and Forest Meteorology*, vol. 232, pp. 225–234, 2017.

[32] S. Liu, J. Y. Yang, X. Y. Zhang, C. F. Drury, W. D. Reynolds, and G. Hoogenboom, "Modelling crop yield, soil water content and soil temperature for a soybean-maize rotation under conventional and conservation tillage systems in Northeast China," *Agricultural Water Management*, vol. 123, pp. 32–44, 2013.

[33] E. Guzev, G. Luboshits, S. Bunimovich-Mendrazitsky, and M. A. Firer, "Experimental validation of a mathematical model to describe the drug cytotoxicity of leukemic cells," *Symmetry (Basel)*, vol. 13, no. 10, pp. 1–17, 2021.

[34] C. Windt, J. Davidson, E. J. Ransley, D. Greaves, M. Jakobsen, M. Kramer, et al., "Validation of a CFD-based numerical wave tank model for the power production assessment of the wavestar ocean wave energy converter," *Renewable Energy*, vol. 146, pp. 2499–2516, 2020.

[35] P. D. Jamieson, J. R. Porter, and D. R. Wilson, "A test of the computer simulation model ARCWHEAT1 on wheat crops grown in New Zealand," *Field Crops Research*, vol. 27, no. 4, pp. 337–350, 1991.

[36] L. Zhang, X. Deng, W. Li, Y. Ding, R. Chi, and X. Zuo, "Kinetics of weathered-crust elution-deposited rare-earth ore in a leaching process," *Materials Technology*, vol. 47, no. 2, pp. 145–148, 2013.